

Neural Network Estimation of Particle Size Distribution Parameters in Ice-phase Clouds Using Three Frequency Radar Measurements

S. M. Sekelsky and R. E. McIntosh
Microwave Remote Sensing Laboratory
University of Massachusetts at Amherst
Amherst, Massachusetts

W. L. Ecklund
Cooperative Institute for Research in Environmental Sciences
University of Colorado
Boulder, Colorado

K. S. Gage
National Oceanic and Atmospheric Administration
Aeronomy Laboratory
Boulder, Colorado

Introduction

Lidar and IR radiometric particle sizing techniques are affected by high extinction rates. Thus, they cannot be used for ground-based remote sensing of effective particle size in optically thick clouds or when low liquid water clouds or precipitating clouds are present. On the other hand, modern ground-based millimeter-wavelength radars are sensitive to cloud particles and can penetrate most clouds, even precipitating clouds. Millimeter-wavelength systems also experience non-Rayleigh scattering that can be exploited to form estimates of particle size distribution characteristics when used as part of a multi-wavelength radar (Lhermitte 1987; Matrosov 1993; Sekelsky and McIntosh 1996).

This publication describes a neural network that combines simultaneous reflectivity measurements from three radar wavelengths to estimate effective particle size and peak number concentration in clouds composed of dry ice particles. It presents radar measurements collected during the Maritime Continent Thunderstorm Experiment (MCTEX). During November and December 1995, the University of Massachusetts (UMass) Cloud Profiling Radar System (CPRS) and the National Oceanic and Atmospheric Administration (NOAA) Aeronomy Laboratory S-band Profiler were deployed next to each other at Garden Point, Melville Island, Australia. The UMass radar operates at 3.16 mm (W-band) and 9.06 mm (Ka-band) and uses a single 1-m-diameter

aperture to ensure beam collocation. The NOAA system operates at 10.6 cm (S-band) and uses a single 3-m-diameter antenna. Attenuation at S-band is negligible over the path lengths considered, and S-band data are used to resolve ambiguities between attenuation and non-Rayleigh scattering. Initial results for stratiform clouds show a characteristic decrease in particle diameter with height. No trend is observed for the convective case.

Neural Network

Although two wavelengths are required to estimate effective particle size and peak number concentration, reflectivity data collected at three wavelengths can be combined to provide more precise estimates over a larger range of particle diameters. To combine this information, multivariate regression analysis was attempted but was numerically unstable because of its high order and was difficult to modify because of its complexity. In contrast, the neural network solution described here is easily modified and more stable over a wide range of input values. Neural networks can model any function that can be described by classical methods; and they hide the complexity of input-output relationships, freeing the user from details of implementation. Neural networks have been used to classify cloud type (Lohmeier et al. 1997; Xiao and Chandrasekar 1997) and other quantitative parameters from remotely sensed data.

Figure 1 shows a neural network consisting of four layers: 1) a layer containing three input nodes, 2) a layer of seven hidden nodes, 3) a second hidden layer of four nodes, and 4) a layer of two output nodes. The input vector, \bar{X} , is

$$\bar{X} = \frac{1}{100} [DW R_{S,W}, DW R_{Ka,W}, dBZ_{e,W}], \quad (1)$$

where the dual-wavelength ratio, DWR, is defined by

$$DW R_{l,s} = 10 \log \left(\frac{Z_{e,l}}{Z_{e,s}} \right) \quad (2)$$

Z_e has units of $mm^6 m^{-3}$, l denotes the longer-wavelength radar band and s denotes the shorter-wavelength band. Note that Equation (2) assumes volume-mismatch and attenuation effects have been removed from $Z_{e,l}$ and $Z_{e,s}$.

Elements of the input vector, \bar{X} , were chosen for their physical relationship to the outputs, but are equivalent to inputting the three radar reflectivities. Scaled logarithmic values are used to reduce the dynamic range of values that must be modeled by the neural network. The output vector, \bar{Y} , includes two parameters of a Gamma particle size distribution:

$$\bar{Y} = \frac{1}{100} [\log(N_o), D_m], \quad (3)$$

where $N(D) = N_o \text{Dexp}(-4.67D/D_m)$ is the Gamma particle size distribution with a shape factor of 1.

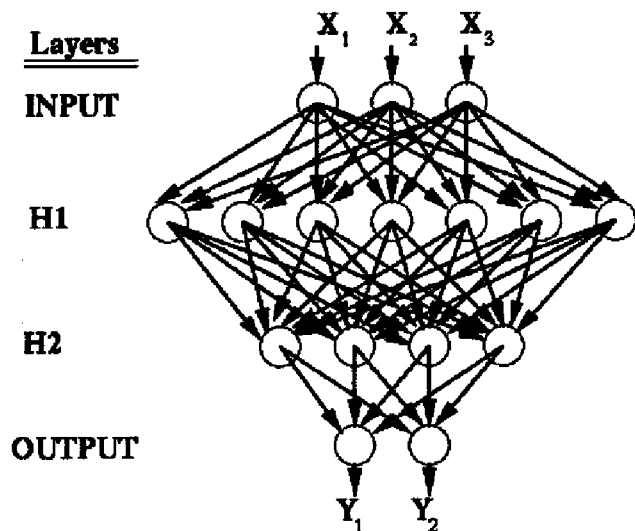


Figure 1. Neural network used to estimate D_m and N_o . See text for details.

Training Data

In order to form the neural network, it must be trained with input vectors, \bar{X} , and corresponding, known output vectors, \bar{Y} . Our network was implemented using the Stuttgart Neural Network Simulator version 4.1 (Zell et al. 1995) and trained with simulated data. Standard back propagation was used to train the neural network.

Figure 2 plots a model of DWR versus effective diameter, D_m . The model assumes dry spherical ice particles with a size-density relationship, $D[gcm^{-3}] = 0.7/D[mm]$ given by Klassen (1988). As suggested by Klassen, the range of D is limited so that $0.005 < D < 0.9 [gcm^{-3}]$. Backscatter cross-sections used in training data for the neural network were calculated with the discrete-dipole approximation (DDA) using the DDSCAT (V5a) software package (Draine and Flatau 1996). Errors in reflectivity are negligible for distributions of particles having effective particle diameters as large as 10 mm.

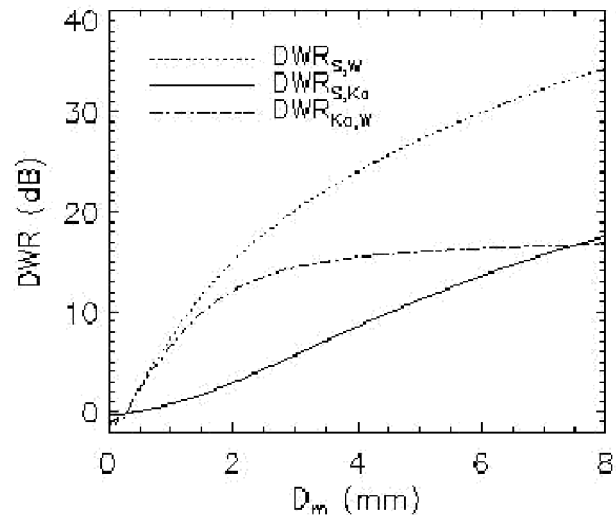


Figure 2. Dual-wavelength-ratio (DWR) as a function of effective particle diameter for dry ice. The model assumes a Gamma distribution of spheres.

Results

Figures 3a and 3b show histograms of median particle diameter for stratiform and convective cloud conditions, respectively. The cloud data used to create these figures was edited to remove consideration of precipitation and the melting layer thus the first range gate is at approximately 4.2 km above ground level.

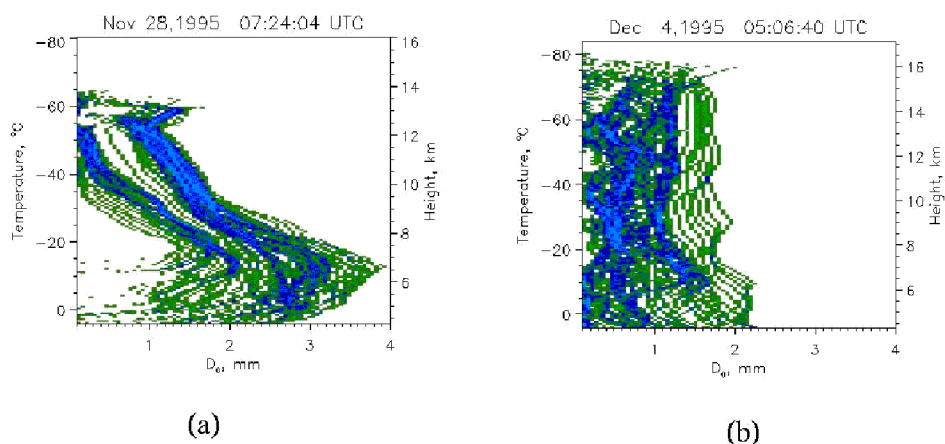


Figure 3. Histogram of D_m for (a) stratiform and (b) convective clouds.

The contrast between the vertical distribution of particle size is striking. Figure 3a shows that above a certain altitude, D_m monotonically decreases with height for stratiform conditions, while Figure 3b indicates no such trend for the convective case. Measurements presented for the stratiform case were collected beginning about 2½ hours after intense convection and show no substantial up-drafts. To correct for attenuation effects, cloud-top reflectivities were matched at the different frequencies, taking into account differences in the index of refraction for ice and water at the different wavelengths. S-band reflectivity values were used as a reference since the S-band signal is not attenuated.

The convective case occurred within a few minutes of a near miss by a convective cell, but only weak precipitation ($R_r < 1 \text{ mmhr}^{-1}$) fell on the radars. Because features in DWR near cloud-top indicated non-Rayleigh scattering, the cloud-top matching scheme used to remove attenuation for the stratiform case could not be applied here. Instead, a small correction for attenuation was applied using radar-derived rain rates.

References

- Draine, B., and P. Flatau, 1996: *User Guide to the discrete dipole approximation code DDSCAT* (version 5a). Princeton Observatory Preprint, Princeton University, Princeton, New Jersey.
- Klassen, W., 1988: Radar observations and simulation of the melting layer of precipitation. *J. Atmos. Sci.*, **45**, 24, 3741-3753.
- Lhermitte, R. M., 1987: Observations of stratiform rain with 94 GHz and S-band Doppler radar. Technical Report AFGL-TR-0268, Air Force Geophysics Laboratory, Hanscom Air Force Base, Massachusetts.
- Lohmeier, S., S. Sekelsky, and R. E. McIntosh, 1997: Classification of cloud particle types using 33 and 95 GHz polarimetric Doppler radars. *IEEE Trans. Geosci. and Remote Sens.* **35**, 2,256-2,270.
- Matrosov, S., 1993: Possibilities of cirrus particle sizing from dual-frequency radar measurements. *J. Geophys. Res.*, **98**, 11, 20675-20683.
- Sekelsky, S., and R. McIntosh, 1996: Cloud observations with a polarimetric 33 GHz and 95 GHz radar. *Meteorol. Atmos. Phys.*, **58**, 123-140.
- Xiao, R., and V. Chandrasekar, 1997: Development of a neural network based algorithm for rainfall estimation from radar observable. *IEEE Trans. Geosci. and Remote Sens.*, **35**, 1, 160-171.
- Zell, A., G. Maimier, and M. Vogt, 1995: *Stuttgart Neural Network Simulator: User Manual, Version 4.1*. University of Stuttgart, Stuttgart, Germany.